Vol. 68: 169–182, 2016
doi: 10.3354/cr01388

CLIMATE RESEARCH
Clim Res

Published May 4

Contribution to CR Special 32 'CLARIS-La Plata Basin: climate variability and uncertainties'

Changes in precipitation over the La Plata Basin, projected by CLARIS-LPB regional models

Iracema Fonseca de Albuquerque Cavalcanti*, Virginia Piccinini Silveira

Center of Weather Forecasting and Climate Studies/National Institute for Space Research (CPTEC/INPE), Rodovia Presidente Dutra, Km 40, CEP: 12630-000, Cachoeira Paulista, SP, Brazil

ABSTRACT: The La Plata Basin (LPB) is an important region for social and economic sectors of South America, mainly as a source of water and for agriculture. Regional models are used to analyze changes in precipitation over South America in order to provide more details of the projected changes in specific regions. Results of regional models from the CLARIS-LPB project are analyzed to assess changes and uncertainties in future projections for the LPB compared to the base period. Results from several models are taken into account in order to assess uncertainties. The models agree in projecting more precipitation in the whole basin and in an increased frequency of extreme wet austral summers. The majority of models agree in projections of drier conditions in the upper LPB and an increase in the frequency of extreme dry austral winters and springs. However, in the lower LPB the projections indicate an increase in the frequency of extreme wet winters and springs. In austral autumn the uncertainties are high in the upper LPB. The uncertainties are low regarding increases in the frequency of rainy days in the middle and lower LPB and in the maximum number of consecutive dry days in the upper LPB. The projected patterns of austral summer anomaly precipitation variability obtained from empirical orthogonal function analysis display the same dipole between southern LPB and the South Atlantic Convergence Zone as in the base period, but increased anomalies in the northern center. In the austral winter the only anomaly signal simulated in the base period remains in the future projections, but the maximum variability is displaced southwards.

KEY WORDS: Precipitation extremes · Regional models · La Plata Basin · Climate change · Frequency of extremes · Precipitation variability · Precipitation indices

1. INTRODUCTION

The La Plata Basin (LPB), located in the southeastern region of South America (SA), comprises areas of Brazil, Argentina, Uruguay and Paraguay. This region is highly populated and has urban and agricultural areas, as well as Itaipu, the largest hydroelectric power plant in SA. Therefore extreme precipitation in the LPB, i.e. excess or deficit of rainfall, can affect the society and the economy of four different countries. Studies using observed precipitation have shown positive trends in extreme rainfall over the LPB. Haylock et al. (2006) used precipitation data sets from stations over SA during the period 1960–2000 to analyze extreme indices over this continent. The results showed significant positive trends in the indices over large areas of the LPB, indicating increases in total precipitation, in the frequency of days with rainfall above 10 and 20 mm d^{-1}, in the number of consecutive wet days, and in consecutive dry days. Using observed precipitation in stations from 1950 to 2010, Skansi et al. (2013) analyzed extreme indices over SA and obtained results similar to Haylock et al. (2006). In addition, analysis of 2 indices by Penalba & Robledo (2010): the percentage of days with rainfall ≥0.1 mm and the 75th percentile of this indicated positive trends in large areas of the LPB between 1961–1975 and 1980–1996. Positive

*Corresponding author: iracema.cavalcanti@cptec.inpe.br

trends in observed extreme precipitation were also detected over southeastern South America by Dufek & Ambrizzi (2008) during the period 1961–1990 and by Re & Barros (2009) during the period 1959–2002.

A review of precipitation extremes over the LPB and results from the CLARIS-LPB project are presented in Cavalcanti et al. (2015), where remote and local influences, as well as extreme indices are discussed based on observations and model results. In that study, analyses of precipitation from the Global Precipitation Climatology Project (GPCP) dataset (Adler et al. 2003) showed that the frequency of wet extremes was higher in the southern sector than in the northern sector of the LPB and that the number of wet cases in both sectors was higher than the number of dry cases. Two global models reproduced this behavior in the period 1979–2001. The highest number of observed dry extremes during the period 1962–2008 was recorded at stations in central Argentina and Paraguay. Moderate to high drought hazard index (DHI) values were recorded in the western and southern LPB. The DHI is a weighted index based on drought frequencies, calculated as a sum of weighted drought classes:

$$DHI = (MD_r \times MD_w) + (SD_r \times SD_w) + (ED_r \times ED_w) \quad (1)$$

where MD, SD and ED are moderate, severe and extreme drought classes from the Standardized Precipitation Index (SPI), w is the weight of the drought class and r indicates the percentage of occurrence. The values of the weights and ratings can be found in Shahid & Behrawan (2008).

Future climate projections of extreme precipitation were discussed in IPCC-AR5 (Christensen et al. 2013) and Kitoh et al. 2013, mainly from a large ensemble of CMIP5 global models. Individual models can show differences in results, and uncertainties have been discussed in some studies. Using 24 CMIP3 models and a criterion of convergence and model bias, Torres & Marengo (2013) concluded that the precipitation uncertainty range over SA had the same magnitude as natural variability. Blázquez & Nunez (2013) analyzed CMIP3 and CMIP5 model results over SA to identify sources of uncertainty and found that the inter-model variability of precipitation during summer decreased from CMIP3 to CMIP5 in north, east and south Brazil and Uruguay, mainly in the last decades of the 21st century. The reduction in inter-model variability was related to a better representation of physical processes in the new generation models of CMIP5.

Results of several regional climate models obtained in American programs — such as the North American Regional Climate Change Assessment Program (NARCCAP; Mearns et al. 2012) for North America and CLARIS-EU and CLARIS-LPB (Boulanger et al. 2010) for South America — have been used for similar purposes. One of the most important functions of these programs is to provide climate change information with a high resolution that can be used in assessment of climate impacts and adaptation needs. For South America, experiments have been performed to enhance the details of precipitation changes. Marengo et al. (2012) and Chou et al. (2012) analyzed 4 members of the regional Eta model integrated with lateral boundary conditions from a global model with different sensitivities to global warming (Murphy et al. 2004). They found that the spread among members was smaller than the precipitation bias. Sources of uncertainties were discussed in Solman & Pessacg (2012), using the regional MM5 model and analyzing the role of initial conditions, the domain of integration and the physical parameters. The experiments were done with a combination of cumulus convection and planetary boundary layer (PBL) schemes. Four convection schemes and 2 PBL schemes testing different maximum lifting depth for an unstable parcel were analyzed. The highest source of uncertainty arose from differences in physical parameters, and the lowest from the initial conditions.

Therefore, different models, which have different parameterizations, are likely to present more spread than a single model with several members. For example, an evaluation of extreme precipitation over southeastern SA, in 4 regional models, showed high uncertainties in large areas of the LPB (Carril et al. 2012). In that study, the model ensemble overestimated the number of wet days and underestimated the intensity of precipitation, when compared to Climatic Research Unit (CRU) and CPC Merged Analysis of Precipitation (CMAP) data.

The objective of the present study is to show the changes in precipitation and extremes projected for the future, compared to a past base period, and to discuss the uncertainties arising from results of different regional models. Different analyses are performed to assess the uncertainties in areas of the LPB. The analyses and discussions consider differences in precipitation and extremes over SA between the future projections and the base period. As the LPB extends from tropical to extratropical regions, the precipitation regimes are different in the northern, middle and southern areas. Therefore the seasonal and daily analyses were performed in 4 locations situated at the upper, middle and lower LPB (Fig. 1).

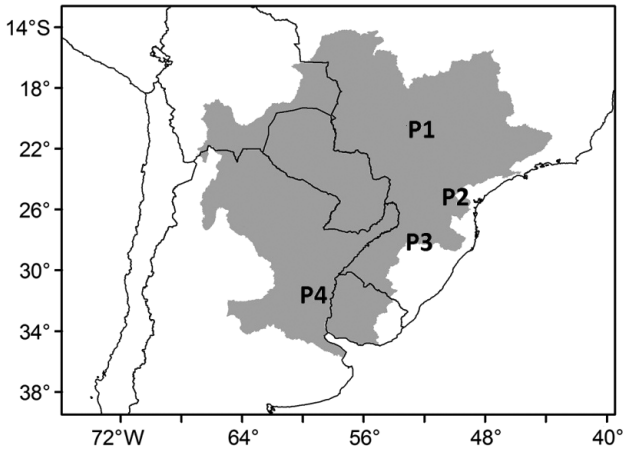

Fig. 1. La Plata Basin (gray) in South America and 4 locations where the changes in model precipitation were analyzed

2. DATA AND METHODS

The simulations and projections were obtained from 5 regional models provided by the CLARIS-LPB project: Eta (Chou et al. 2012), LMDZ (Hourdin et al. 2006), PROMES (Sánchez et al. 2004), RCA (Samuelsson et al. 2011) and RegCM3 (da Rocha et al. 2009). The integrations were performed over the South American domain, with 50 km horizontal resolution. A previous evaluation of these models demonstrated that they reproduce the spatial distribution of seasonal variability, and that there is a low degree of spread among the model results over most of SA, except over the Andes mountain range (Solman et al. 2013). Observed precipitation extremes for the LPB have been analyzed in other studies, described in Cavalcanti et al. (2015). Therefore, in the present analyses, only model results are discussed. The base period is 1961–1988, and this is compared with the distant future period 2071–2098. PROMES and ETA models were forced by the HadCM3 coupled general circulation model (CGCM), the LMDZ model was forced by IPSL CGCM, and RCA and RegCM3 models were forced by ECHAM5 CGCM (Table 1). More information about these simulations can be found in Carril et al. (2012), Solman et al. (2013), Cavalcanti et al. (2015) and Sánchez et al. (2015). The RegCM3 model is used only for the daily analyses, due to the smaller period of available data in future projection (2071–2096). All global models for the downscaling were obtained from the CMIP3 integrations of base period and future projections with scenario A1B (Nakicenovic et al. 2000).

The differences between the future and base periods are analyzed in the model ensemble, and the spread among the models is obtained from the standard deviation among them. Four specific areas within the basin are analyzed, each comprising an average of 9 grid points, where the central grid point is P1 (52.25° W, 19.75° S), P2 (49.75° W, 25.25° S), P3 (52.75° W, 27.75° S) and P4 (59.75° W, 31.75° S), shown in Fig. 1. These areas were chosen to represent the upper LPB (P1), middle LPB (P2 and P3) and lower LPB (P4), and also to cover areas which are frequently affected by floods. The percentages of changes in these regions are analyzed for each model in the 4 seasons. The frequencies of seasonal precipitation extremes are calculated through the 5th, 10th and 25th

Table 1. Climate models used for investigation of projected changes in precipitation over the La Plata Basin (adapted from Solman et al. 2013 and Sánchez et al. 2015)

Model	Responsible institute	Type of grid	Number of grid points	Number of levels	Global model	Basic Reference	
						Regional	Global
ETA/INPE (climate change V1.0)	Instituto Nacional de Pesquisas Espaciais, Brazil	Regular lat/lon	123 × 245	38	HadCM3-Q0	Chou et al. (2012)	Gordon et al. (2000)
LMDZ4	Institute Pierre-Simon Laplace, France (IPSL)	Irregular rectangular lat/lon	184 × 180	19	IPSL-CM4-v2	Hourdin et al. (2006)	Marti et al. (2010)
PROMES	Universidad Castilla, La Mancha, Spain (UCLM)	Lambert conformal	145 × 163	37	HadCM3-Q0	Sanchez et al. (2004)	Gordon et al. (2000)
RCA3	Rossby Centre Meteorological and Hydrological Institute, Sweden (SMHI)	Rotated lat/lon	134 × 155	40	ECHAM5-OM	Samuelsson et al. (2011)	Roeckner et al. (2006)
RegCM3	Universidade de São Paulo, Brazil (USP)	Rotated Mercator	190 × 202	18	ECHAM5-OM	da Rocha et al. (2009)	Roeckner et al. (2006)

percentiles (dry cases), and the 75th, 90th and 95th percentiles (wet cases) in the base and future periods. The frequency in the future period is analyzed relative to the percentiles of the base period. Normally, percentile analyses are performed to identify daily extremes, but here the method is applied to seasonal precipitation, which is also important for agriculture and water resources management. We analyze the difference between the future and the base periods in the 4 seasons and for the 4 locations.

Daily precipitation is used to calculate the indices SDII (mean precipitation of rainy days, i.e. with precipitation ≥1 mm d^{-1}) and CDD (maximum number of consecutive dry days) for the 4 locations in the LPB. In order to detect differences in the main mode of precipitation variability between the 2 periods (base and future), empirical orthogonal function (EOF) analysis was applied to standardized precipitation anomalies obtained from the 4 regional models in the LPB domain.

In addition to the spread of results from different regional models, which have different physical parameterizations, the lateral boundary conditions provided from different global models are a further source of uncertainty. However in the present analyses uncertainty is defined based on the amount of spread among models results, as high (large spread) or low (agreement among models). In the maps of differences between future projections and base period it is measured by comparing the signs of precipitation change (positive or negative) and the standard deviation among the models. If the signs are the same, and the standard deviation is small, the uncertainty is considered low.

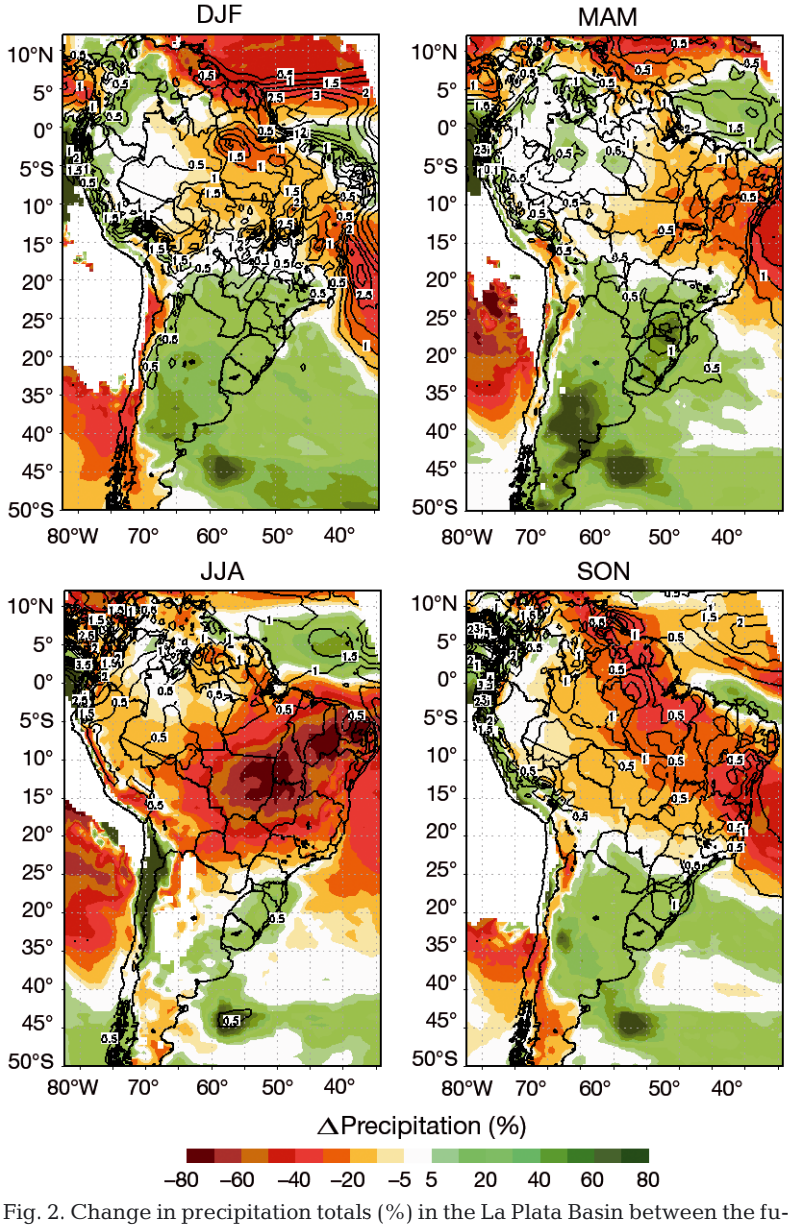

Fig. 2. Change in precipitation totals (%) in the La Plata Basin between the future period (2071–2098) and the base period (1961–1988). Contour lines show the standard deviation among the climate models

3. SEASONAL PRECIPITATION CHANGES OVER SOUTH AMERICA AND MODEL DISPERSION

Changes in future precipitation in percentages relative to the base period during the 4 seasons over the entire LPB are shown in Fig. 2. In general, the ensemble projects more precipitation over the LPB in the future, during DJF (austral summer) and MAM (austral autumn), but drier conditions over the northern sector (ca. 15° to 23° S) and wetter conditions over the southern sector (ca. 25° to 35° S) are projected during JJA (austral winter) and SON (austral spring). Some of these features are also displayed in results of CMIP5 global models (Cavalcanti & Shimizu 2012, Christensen et al. 2013), as well as in regional models such as the Eta model (Marengo et al. 2012).

During DJF, the ensemble indicates positive values in the majority of the LPB, with low standard deviation, expressing low uncertainty regarding increased precipitation over the region

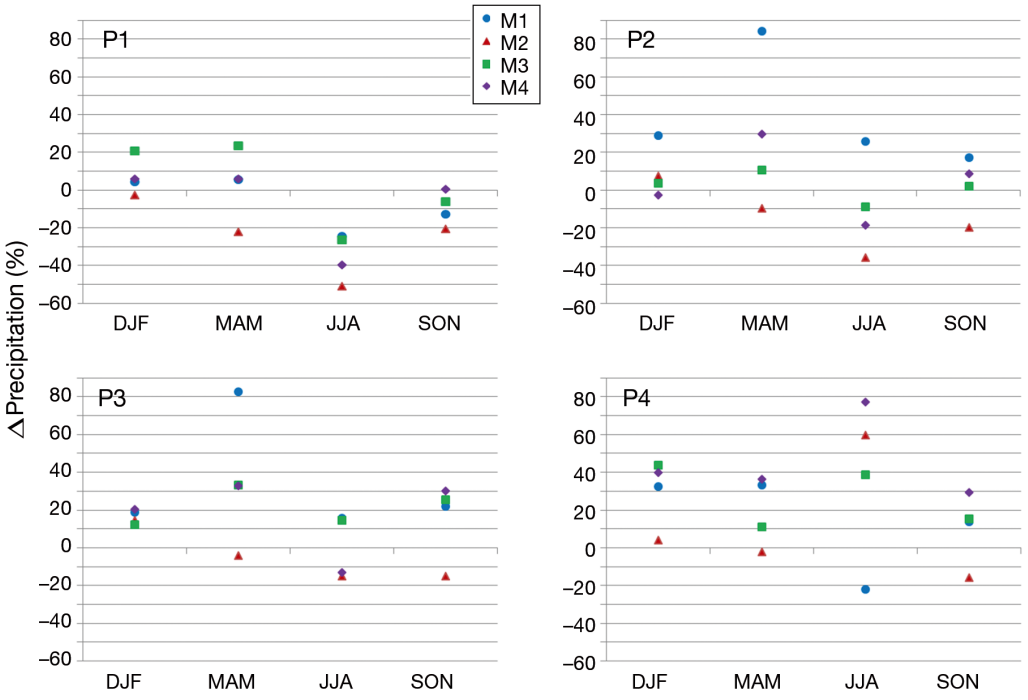

Fig. 3. Seasonal changes in precipitation projected by 4 regional climate models in the La Plata Basin between the future period (2071–2098) and the base period (1961–1988), at the 4 locations (P1–P4) shown in Fig. 1. M1: ETA, M2: LMDZ, M3: PROMES, M4: RCA

in the future period. There is also low uncertainty regarding drier conditions in the future over the northern LPB, projected in the ensemble during JJA and SON. Over the southern sector the projections show increased precipitation in JJA and SON, with low uncertainty, since there are positive values in the ensemble and small standard deviations. The impact of global model resolution on increased precipitation over central LPB in the future is smaller in SON than in the other seasons, as shown in Blázquez et al. (2012) who compare results from MRI at 20 km vs. 60 km resolutions. In that study they found that the most significant precipitation increase in southeastern SA was projected for the spring.

In MAM, the standard deviation among the models (shown by contour lines in Fig. 2) is higher over the LPB than in the other seasons and, although the projection indicates increased precipitation over this region, the uncertainty is higher than in the other seasons. The results for DJF and JJA are consistent with those from a larger set of regional models, shown in AR5-IPCC, which includes the models analyzed here (Fig. 14.21 in Christensen et al. 2013). These results indicate agreement among models regarding increased precipitation in southeastern SA in DJF. The reduced precipitation over the northern sector of the LPB during JJA was also noted by Christensen et al. (2013). The general configuration of precipitation changes in DJF and JJA are also similar to results using 1 regional model (Eta) and an ensemble of 4 members shown in Marengo et al. (2012), although the magnitude of changes is higher in that study, where the different members were integrated with different lateral boundary conditions from the HadCM3 global model. In the present study, the ensemble of different models with different lateral boundary conditions, different parameterizations and different configurations gives a lower percentage of precipitation change.

The percentages of changes with respect to the base period projected by the individual members are shown in Fig. 3, for the 4 areas (locations) with central points at P1, P2, P3 and P4 indicated in Fig. 1. In DJF at least 3 members show positive changes during DJF in the 4 locations. By contrast, negative changes and reduced precipitation in the future are projected by the 4 models at P1 (upper LPB) during JJA. In the middle LPB, 3 models project reductions during JJA at P2 and there is high uncertainty at P3, as 2 models show an increase and 2 show a reduction. However, at P4, 3 models show increased precipitation in JJA. Three models project increased precipitation during MAM in the 4 locations and during SON at P2, P3 and P4. The reduction of precipitation in the future compared to the base period in SON at P1 would indicate a longer dry season, which

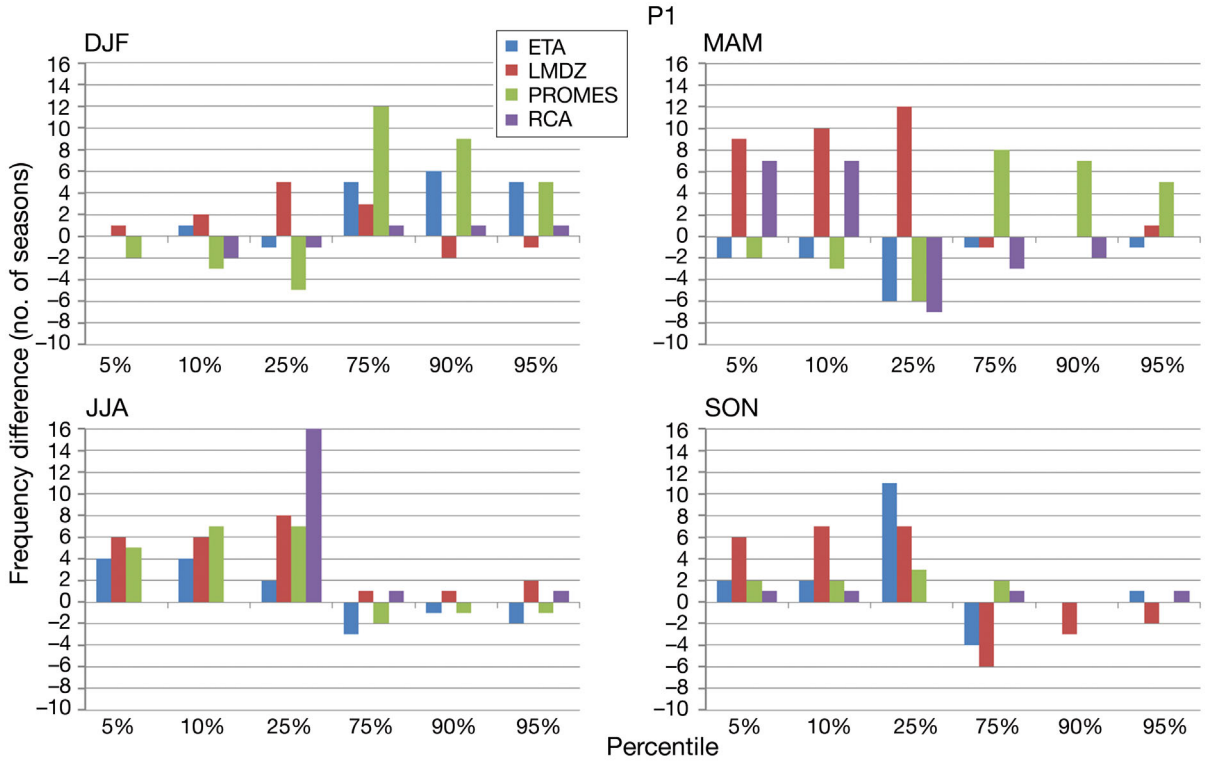

Fig. 4. Differences in the number of extreme dry (5th, 10th and 25th percentiles) and extreme wet (75th, 90th and 95th percentiles) years between the future period (2071–2098) and the base period (1961–1988) at location P1, for each season, simulated by 4 regional climate models. DJF: austral summer; MAM: autumn; JJA: winter; SON: spring

occurs in JJA, affecting the onset of the South American monsoon System (SAMS). Drier conditions in the future SAMS, during the austral spring, were also obtained by Seth et al. (2010, 2011).

In summary, there is low uncertainty regarding increased precipitation in the entire LPB during DJF and reduced precipitation in the northern sector, but an increase in the southern sector, during JJA. The uncertainties are higher in the middle LPB sector during JJA. The uncertainties are low during SON in the LPB, where the projections indicate reduced precipitation in the northern sector and increased precipitation in the middle and southern sectors. Even though in MAM 3 out of 4 models show increased precipitation in the 4 locations of LPB, the dispersion is larger than in the other seasons.

4. PRECIPITATION EXTREMES

4.1. Frequency of seasonal extremes from percentiles

The uncertainties are discussed based on the agreement or disagreement among the models with respect to the difference between the number of seasonal precipitation extremes in the future and base periods. Frequency extremes are computed with respect to the seasonal precipitation for each year. For example, a wet extreme in the austral summer is identified as a year in which the seasonal DJF precipitation exceeds the 75th, 90th, or 95th percentile of the whole series of 28 years. The number of extremes in the future is calculated considering the percentiles of the base period. Figs. 4–7 show the difference in the number of dry extremes (5th, 10th, or 25th percentile) and wet extremes (75th, 90th or 95th percentile) in the 4 areas and 4 seasons.

At P1 (Fig. 4), during DJF the frequencies of wet extremes in the future are higher than in the base period for the 3 percentiles. All models show increased frequency of wet extremes in the 75th percentile and at least 3 out of 4 models also show increases in the 90th and 95th percentiles. Three models project a reduction in the frequency of dry extremes in the 25th percentile, while there are more uncertainties in the 5th and 10th percentiles. The increased frequency of wet extremes during summer might indicate heavier daily rainfall or continuous rainfall in the South Atlantic Convergence Zone (SACZ), both of which would increase the risk of flooding and landslides in the region. In MAM, only

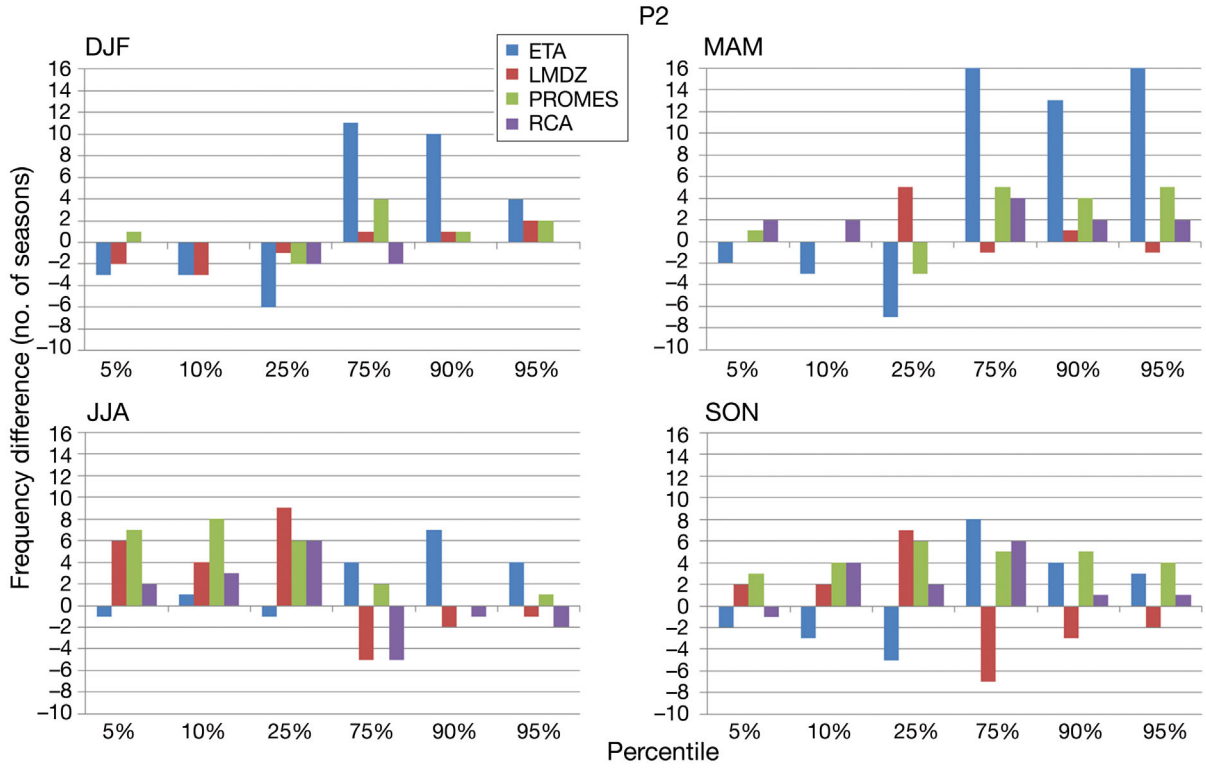

Fig. 5. Differences in the number of extreme dry (5th, 10th and 25th percentiles) and extreme wet (75th, 90th and 95th percentiles) years between the future period (2071–2098) and the base period (1961–1988) at location P2, for each season, simulated by 4 regional climate models

1 model shows increased frequency of wet extremes in the 3 percentiles, and 3 models show a reduction in the frequency of dry extremes in the 25th percentile. The models do not agree in the sign changes; therefore in MAM the uncertainty is high. In JJA and SON there is a clear increase in the frequency of dry extremes in the future, compared to the base period, and there is great agreement among the models. The changes are very small for the wet extremes in JJA, and 1 model shows reduced frequency of wet extremes in the 3 percentiles in SON. At P2 (Fig. 5), there are increases in the frequency of wet extremes in DJF and MAM in the majority of future projections, while there is a reduction in the frequency of dry extremes in DJF in the 3 percentiles. In JJA there is agreement among models regarding increased frequency of dry extremes. In SON there is a general increase in the frequency of both dry and wet extremes in the majority of models.

At P3 (Fig. 6), the frequency of wet extremes in the 3 percentiles increases in the future during DJF, MAM and SON. In DJF the 4 models show increased frequency of wet extremes and a reduction in the frequency of dry extremes. In the other 2 seasons, the majority of models display the same behavior. In JJA the frequency of dry extremes in the future is higher than in the base period, while the models do not agree on the changes in the frequency of wet extremes. At P4 (Fig. 7), there are increases in the frequency of wet extremes during the 4 seasons in the 3 percentiles and a general decrease in the frequency of dry extremes. The increases are projected by all 4 models during MAM and SON and by 3 out of 4 models in DJF and JJA. The behavior at this location in JJA is different from that in the other areas to the north, where there was increased frequency of dry extremes in this season. The increased frequency of wet extremes in DJF at this location is larger than at the other analyzed locations.

The increased frequency of wet extremes in the southern region can be related to an increased moisture flux from Amazonia southwards in future projections, as discussed by Soares & Marengo (2009). The region is also affected by frontal systems, which can be intensified by humidity flux from Amazonia (Siqueira & Machado 2004). Results of 2 global models indicated an increase in the frequency of frontal systems over the LPB in global warming scenarios (Andrade et al. 2012), which could bring more precipitation to the southern region.

Summarizing, comparing the future with the base period, the models show agreement regarding in-

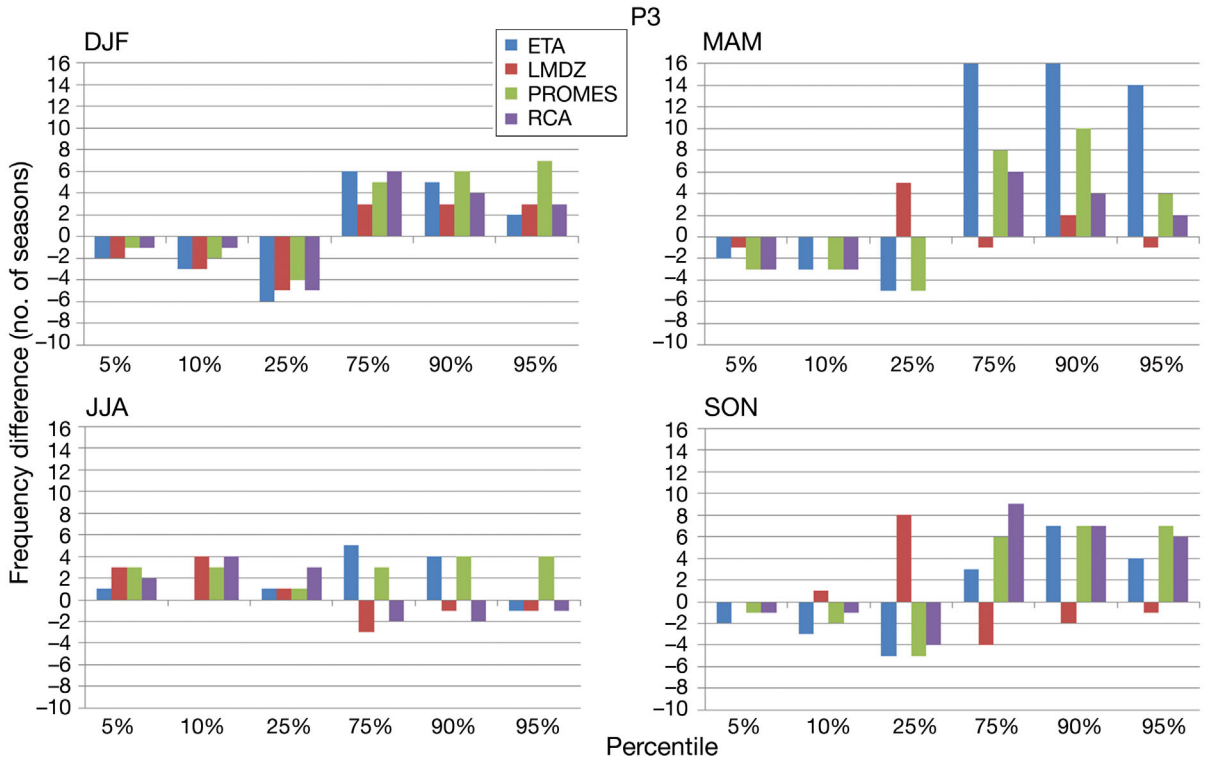

Fig. 6. Differences in the number of extreme dry (5th, 10th and 25th percentiles) and extreme wet (75th, 90th and 95th percentiles) years between the future period (2071–2098) and the base period (1961–1988) at location P3, for each season, simulated by 4 regional climate models

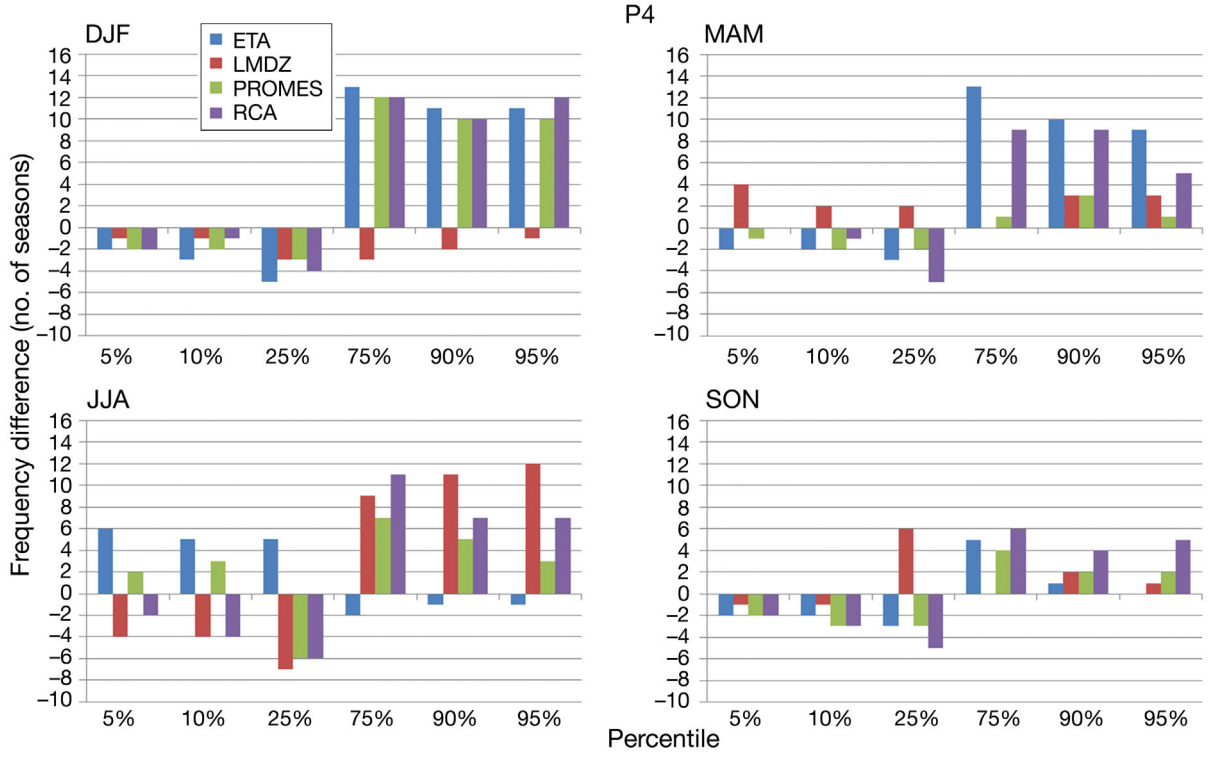

Fig. 7. Differences in the number of extreme dry (5th, 10th and 25th percentiles) and extreme wet (75th, 90th and 95th percentiles) years between the future period (2071–2098) and the base period (1961–1988) at location P4, for each season, simulated by 4 regional climate models

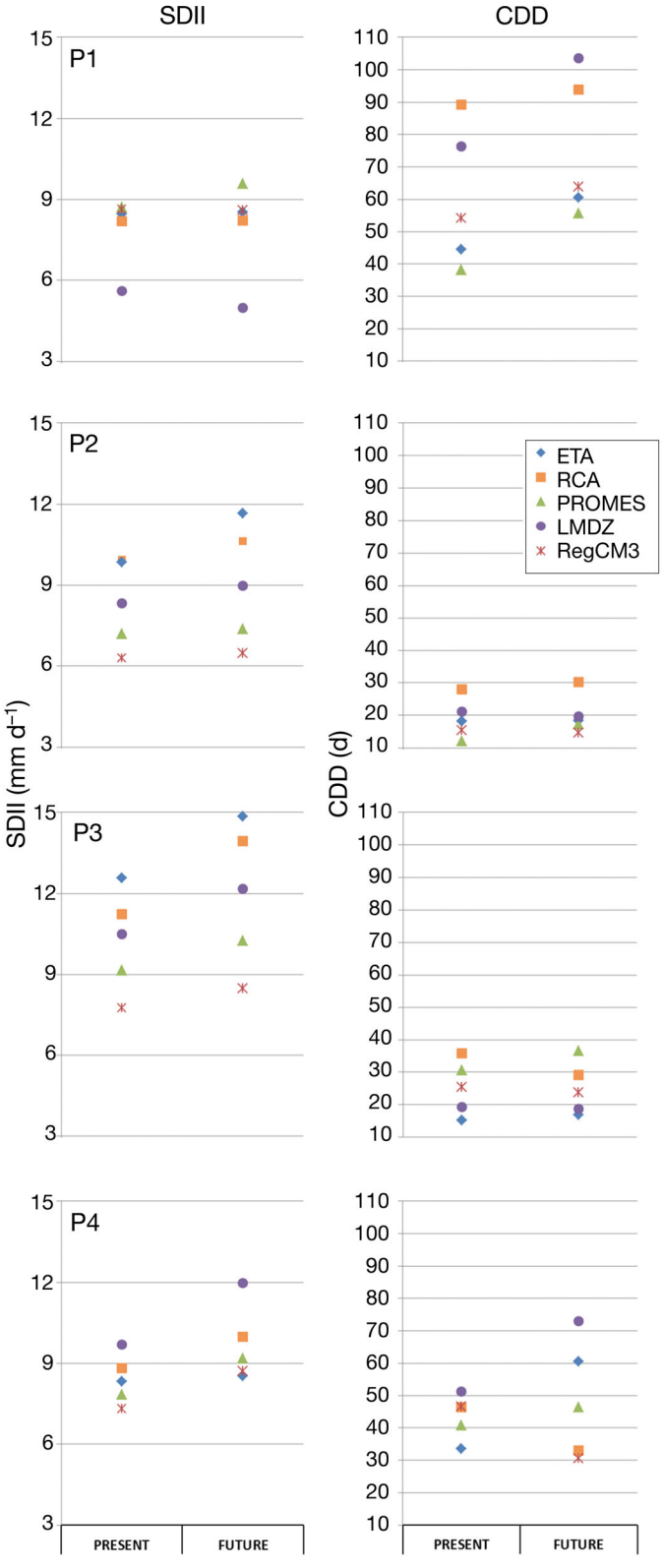

Fig. 8. Precipitation indices SDII and CDD (maximum number of consecutive dry days) simulated by 5 regional climate models at locations P1–P4 in the La Plata Basin (see Fig. 1). Present: 1961–1986; future: 2071–2096

creased frequency of wet extremes frequencies during DJF in the entire LPB, and increases in frequency of dry extremes in JJA in the upper and middle LPB. In SON the behavior is different in each region, with a higher frequency of dry extremes in the upper and middle LPB, and of wet extremes in the lower LPB. During MAM, the middle and lower LPB show increased frequency of wet extremes, while in the upper LPB the uncertainty is high, as there is large spread among the models.

4.2. Daily precipitation indices

Fig. 8 shows values of the SDII and CDD indices for the 4 locations of the LPB. These analyses included the RegCM3 model, in addition to the 4 used to analyze precipitation extremes, and the periods considered were 1961–1986 for the base line period and 2071–2076 for the future, in accordance with data availability. The 5 models project an increase of SDII in P2, P3 and P4 and an increase of CDD in P1, albeit with large model spread in each period. In P2 and P3 the changes in CDD are small. In P4, 3 models show an increase and 2 show a decrease of CDD, indicating more uncertainty than at the other locations. The highest values of CDD are for P1, where the members simulate an interval of ~40 to ~90 consecutive dry days for the base period and ~55 to ~100 d for the future. The lowest values of CDD are for P3, i.e. ~15 to ~35 d in the base period and ~20 to~ 35 d in the future. The results for the 2 periods showed similar behavior to the observed indices analyzed in Skansi et al. (2013) for the period 1950–2010. In addition, the daily indices display the same behavior of mean precipitation during JJA and SON, i.e. drier conditions in the future at the upper LPB and wetter conditions at the middle and lower LPB.

4.3. Anomalous precipitation variability

An EOF analysis of standardized precipitation anomalies over the LPB region reveals the similarities and differences in the main mode of variability (EOF1) among the model results for the base and future periods (Table 2). The spread of variance during the austral summer in both periods and during austral spring during the base period are lower than the spread in austral autumn and winter in both periods. However the spread during summer and winter in the future is similar to the spread in the base period, while in autumn and spring the spread

in the future is larger than in the base period. This is related to the interannual variability represented by the models in each season.

The patterns of EOF1 for each model in the austral summer and winter in both periods are shown in Figs. 9–10. In DJF (1961–1988) the general patterns of the models represent the precipitation dipole over Southeastern SA, as observed in several studies including Nogués-Paegle & Mo (1997), Cunningham & Cavalcanti (2006) and Carvalho et al. (2002) (Fig. 9). This dipole pattern is shown by several global circulation models of CMIP3 in Junquas et al. (2012) and also by HadCM3 GCM in Cavalcanti & Shimizu (2012). In our results, the dipole pattern remains in the future projection, but the intensity of the northern center is higher, indicating stronger anomalies in the SACZ. By contrast, the HadCM3 indicates stronger anomalies in the southern center in future projections, but based on daily anomalies (Cavalcanti & Shimizu 2012). A dipole precipitation pattern was also obtained in a multimodel projection, which showed a preference, in the future, for an increase of events in the positive phase, i.e. positive anomalies in the southern sector of the dipole (Junquas et al. 2012). In JJA the regional models show the same anomaly signal in the whole region in both periods, with a shifting of the maximum southwards (Fig. 10).

In MAM, the models show different patterns for the base period, changing the position of the maximum anomaly of each model in the future projections (not shown). In SON, the models show dipole patterns in the base period, which remain in the future in projections of 2 models, while changing to an unique anomaly signal in the other 2 models (not shown). The time series of principal components, which give the sign of anomalies, indicate interannual variability in the base period and future projections, with agreement among models in some years (not shown).

Table 2. Variance (%) of EOF1 explained by different models used to project changes in precipitation over La Plata Basin

Model	DJF		MAM		JJA		SON	
	Base	Future	Base	Future	Base	Future	Base	Future
ETA	22.5	21.6	38.7	27.2	40.2	33.8	19.6	21.8
LMDZ	18.9	17.5	16.9	15.3	24.5	25.78	18.9	18.9
PROMES	19.3	18.1	19.3	18.7	24.9	42.2	17.5	30.7
RCA	15.3	22.6	25.0	24.7	19.5	24.15	20.8	18.43

5. CONCLUSION

Model projections of precipitation changes in the future, unlike those for temperature, contain uncertainties. An increase in temperature is projected for the entire globe, including SA during the whole year, in global and regional models (Collins et al. 2013, Marengo et al. 2012). In contrast, projected changes in amounts and extremes of precipitation present uncertainties in some regions and seasons. Uncertainties arise from various sources, but in the present study they are analyzed based on the spread of results of different regional models. The projections of different regional models of CLARIS-LPB for the LPB show increased precipitation in the whole basin during DJF, projected by the 4 models, with a low degree of spread among model results indicating a low level of uncertainty. There is also a low level of uncertainty regarding reduced precipitation in the northern sector and increased precipitation in the southern sector during JJA and SON. In MAM the spread among models is larger than in the other seasons.

Changes in extreme seasonal precipitation frequency obtained from percentiles of dry and wet extremes, from base to the future periods, indicate increases in the number of extreme wet summers in the entire LPB, with low uncertainty. Increases in the number of extreme dry winters and springs are also projected in the upper LPB with low uncertainty, while during MAM the uncertainty is high in this region. The region that presents the lowest uncertainty during all seasons is the lower LPB, where the majority of models project increased frequency of seasonal wet extremes. In the middle LPB the majority of models project increased frequency of seasonal wet extremes during MAM and reduced frequency in JJA and SON, also with low uncertainties in these seasons in this region. Daily precipitation indices show rainy days with higher precipitation in the future, mainly in the middle and lower LPB, and increased length of dry periods (consecutive dry days) in the upper LPB.

The models simulate features similar to those identified in observations of the dominant mode of precipitation variability (EOF1). The patterns in the future projections continue to show the dipole precipitation pattern in DJF and the same configuration anomaly in the whole LPB during JJA, as in the base period. The future projections, compared to the base period, present stronger anomalies in the northern summer dipole and a southward shift of the maxi-

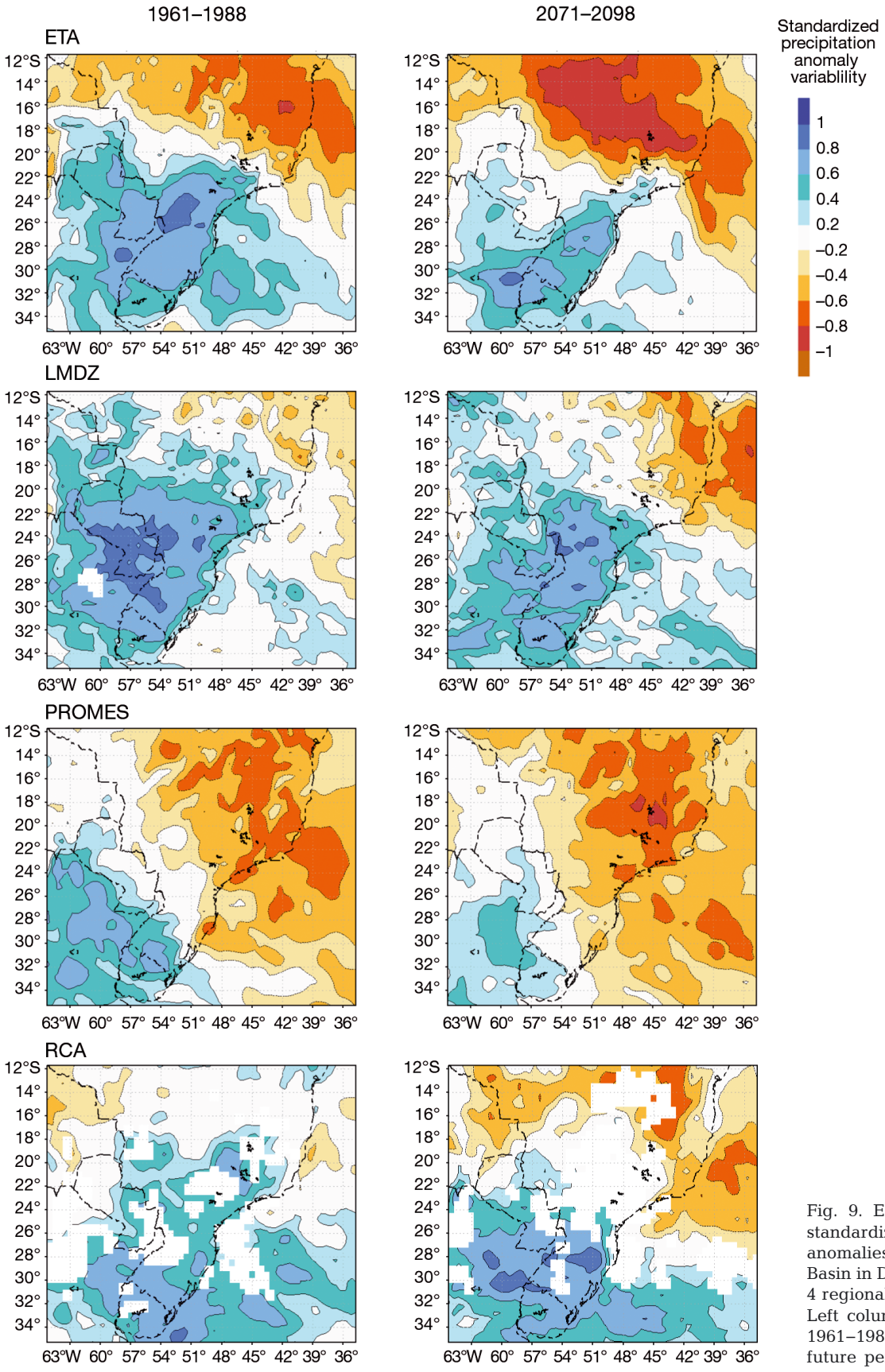

Fig. 9. EOF1 patterns of standardized precipitation anomalies in the La Plata Basin in DJF, simulated by 4 regional climate models. Left column: base period, 1961–1988; right column: future period, 2071–2098)

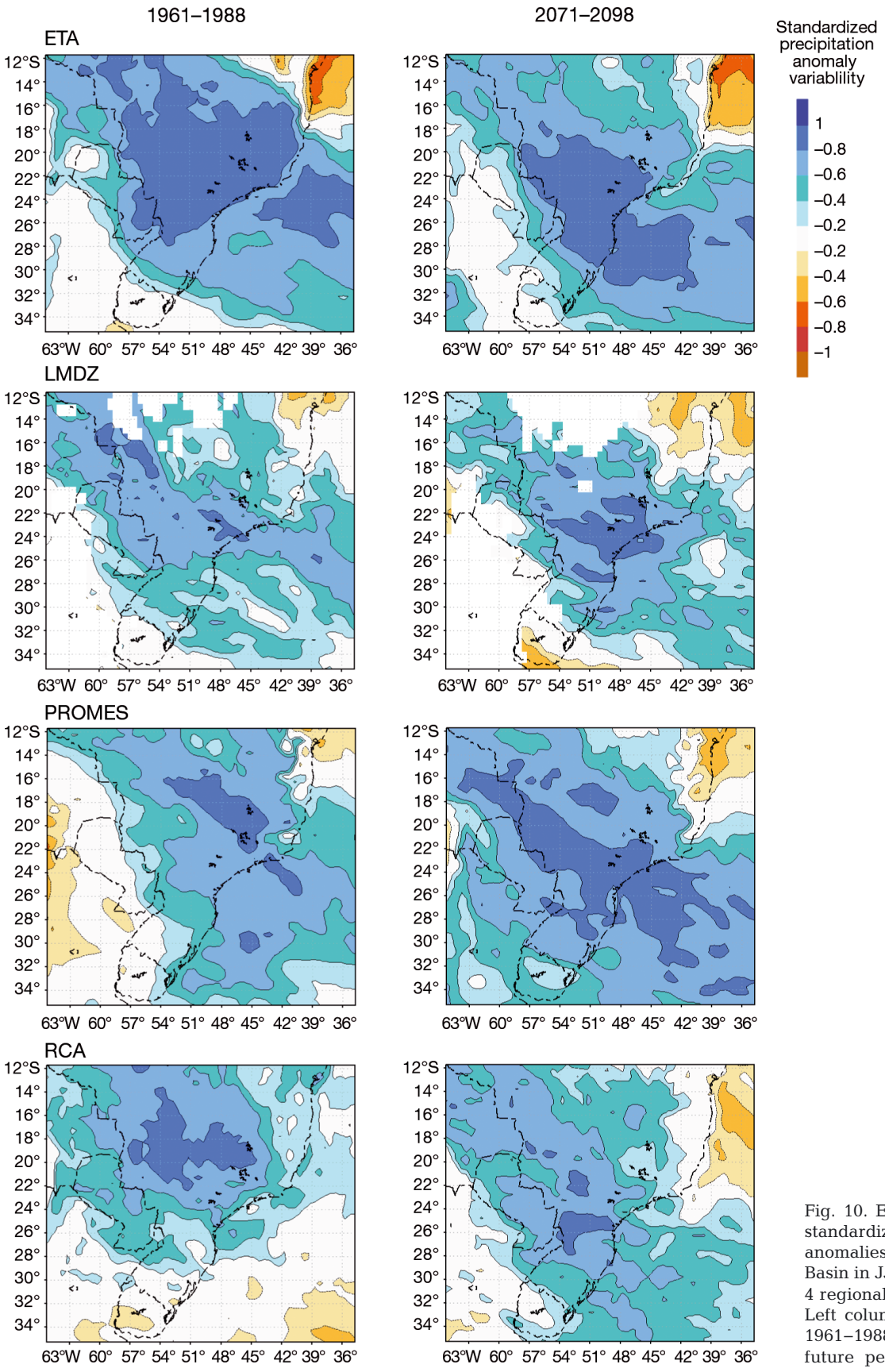

Fig. 10. EOF1 patterns of standardized precipitation anomalies in the La Plata Basin in JJA, simulated by 4 regional climate models. Left column: base period, 1961–1988; right column: future period, 2071–2098

mum anomaly in the winter. In MAM the models show different patterns in the base and future periods, while in SON there is more agreement among models in the base than in the future period.

The results showed changes in mean precipitation, precipitation extremes and patterns of variability projected by 4 regional models, information that can be useful for planning and preparing adaptation measures. The uncertainties, measured by the spread among the models, are low in some seasons and regions of LPB. Since these uncertainties arise mainly from differences in physical parameterizations of regional models, from different lateral boundary conditions of global models and model bias, it is expected that improvements in both global and regional models will reduce the uncertainties and provide better information for use in agriculture and water resource management in the LPB region.

Acknowledgements. The research leading to these results received funding from the European Community's Seventh Framework Programme (FP7/2007–2013) under Grant Agreement No. 212492 'CLARIS LPB: a Europe–South America network for climate change assessment and impact studies in La Plata Basin'. The authors are grateful to the National Counsel of Technological and Scientific Development (CNPq), the National Institute of Science and Technology (INCT) and the São Paulo Research Foundation (FAPESP) for their support.

LITERATURE CITED

Adler RF, Huffman GJ, Chang A, Ferraro R and others (2003) The Version 2 Global Precipitation Climatology Project (GPCP) monthly precipitation analysis (1979–present). J Hydrometeorol 4:1147–1167

Andrade KM, Muller, GV, Cavalcanti IFA, Fernandez Long ME, Bidegain M, Berri G (2012) Changes in the frequency of frontal systems over Southern South America in projections of future climate. Meteorologica 37:15–26 (in Portuguese with English Abstract)

Blázquez J, Nunez MN (2013) Analysis of uncertainties in future climate projections for South America: comparison of WCRP-CMIP3 and WCRP-CMIP5 models. Clim Dyn 41:1039–1056

Blázquez J, Nunez MN, Kusunoki S (2012) Climate projections and uncertainties over South America from MRI/JMA global model experiments. Atmos Clim Sci 2:381–400

Boulanger JP, Brasseur G, Carril AF, Castro M and others (2010) The European CLARIS project: a Europe–South America network for climate change assessment and impact studies. Clim Change 98:307–329

Carril AF, Menéndez CG, Remedio ARC, Robledo F and others (2012) Performance of a multi-RCM ensemble for South Eastern South America. Clim Dyn 39:2747–2768

Carvalho LMV, Jones C, Liebmann B (2002) Extreme precipitation events in southeastern South America and large-scale convective patterns in the South Atlantic Convergence Zone. J Clim 15:2377–2394

Cavalcanti IFA, Shimizu MH (2012) Climate fields over South America and variability of SACZ and PSA in HadGEM-ES. Amer J Clim Change 1:132–144

Cavalcanti IFA, Carril AF, Penalba OC, Grimm AM and others (2015) Precipitation extremes over La Plata Basin: review and new results from observations and climate simulations. J Hydrol (Amst) 523:211–230

Chou SC, Marengo JA, Lyra A, Sueiro G and others (2012) Downscaling of South America present climate driven by 4-member HadCM3 runs. Clim Dyn 38:635–653

Christensen JH, Krishna Kumar K, Aldrian E, An SI and others (2013) Climate phenomena and their relevance for future regional climate change. In: Climate change 2013: the physical science basis. Contribution of Working Group I to the fifth assessment report of the Intergovernmental Panel on Climate Change. Cambridge University Press, Cambridge, p 1217–1308

Collins M, Knutti R, Arblaster J, Dufresne JL and others (2013) Long-term climate change: projections, commitments and irreversibility. In: Climate change 2013: the physical science basis. Contribution of Working Group I to the fifth assessment report of the Intergovernmental Panel on Climate Change. Cambridge University Press, Cambridge, p 1029–1136

Cunningham CAC, Cavalcanti IFA (2006) Intraseasonal modes of variability affecting the South Atlantic Convergence Zone. Int J Climatol 26:1165–1180

da Rocha RP, Rodrigues CAM, Cuadra SV, Ambrizzi T (2009) Precipitation diurnal cycle and summer climatology assessment over South America: an evaluation of Regional Climate Model version 3 simulations. J Geophys Res 114:D10108, doi:10.1029/2008JD010212

Dufek AS, Ambrizzi T (2008) Precipitation variability in São Paulo State, Brazil. Theor Appl Climatol 93:167–178

Gordon C, Cooper C, Senior CA, Banks HT and others (2000) The simulation of SST, sea ice extents and ocean heat transports in a version of the Hadley Centre coupled model without flux adjustments. Clim Dyn 16:147–168

Haylock MR, Peterson TC, Alves LM, Ambrizzi T and others (2006) Trends in total and extreme South American rainfall in 1960–2000 and links with sea surface temperature. J Clim 19:1490–1512

Hourdin F, Musat I, Bony S, Braconnot P and others (2006) The LMDZ4 general circulation model: climate performance and sensitivity to parametrized physics with emphasis on tropical convection. Clim Dyn 27:787–813

Junquas C, Vera C, Li L, Le Treut H (2012) Summer precipitation variability over southeastern south America in a global warming scenario. Clim Dyn 38:1867–1883

Kitoh A, Endo H, Krishna Kumar K, Cavalcanti IFA, Goswami P, Zhou T (2013) Monsoons in a changing world: a regional perspective in a global context. J Geophys Res Atmos 118:3053–3065

Marengo JA, Chou SC, Kay G, Alves LM and others (2012) Development of regional future climate change scenarios in South America using the Eta CPTEC/HadCM3 climate change projections: climatology and regional analyses for the Amazon, São Francisco and the Parana River Basins. Clim Dyn 38:1829–1848

Marti O, Braconnot P, Dufresne JL, Benshila R, Bony S and others (2010) Key features of the IPSL ocean model and its sensitivity to atmosphere model and its sensitivity to atmospheric resolution. Clim Dyn 34:1–26

Mearns LO, Arritt R, Biner S, Bukovsky MS and others (2012) The North American regional climate change

assessment program: overview of Phase I results. Bull Am Meteorol Soc 93:1337–1362

Murphy JM, Sexton DMH, Barnett DN, Jones GS, Webb MJ, Collins M, Stainforth DA (2004) Quantification of modelling uncertainties in a large ensemble of climate change simulations. Nature 430:768–772

Nakicenovic N, Swart R (2000) IPCC special report on emissions scenarios. Cambridge University Press, Cambridge

Nogués-Paegle J, Mo KC (1997) Alternating wet and dry conditions over South America during summer. Mon Weather Rev 125:279–291

Penalba OC, Robledo F (2010) Spatial and temporal variability of the frequency of extreme daily rainfall regime in the La Plata Basin during the 20th century. Clim Change 98:531–550

Re M, Barros VR (2009) Extreme rainfalls in SE South America. Clim Change 96:119–136

Roeckner E, Brokopf R, Esch M, Giorgetta M and others (2006) Sensitivity of simulated climate to horizontal and vertical resolution in the ECHAM5 atmosphere model. J Clim 19:3771–3791

Samuelsson P, Jones C, Willén U, Ullerstig A and others (2011) The Rossby Centre regional climate model RCA3: model description and performance. Tellus 63:4–23

Sánchez E, Gallardo C, Gaertner MA, Arribas A, Castro M (2004) Future climate extreme events in the Mediterranean simulated by a regional climate model: a first approach. Global Planet Change 44:163–180

Sánchez E, Solman S, Remedio ARC, Berbery HP and others (2015) Regional climate modelling in CLARIS-LPB: a concerted approach towards twentyfirst century projections of regional temperature and precipitation over South America. Clim Dyn 45:2193–2212

Seth A, Rojas M, Rauscher SA (2010) CMIP3 projected changes in the annual cycle of the South American Monsoon. Clim Change 98:331–357

Seth A, Rauscher SA, Rojas M, Giannini A, Camargo SJ (2011) Enhanced spring convective barrier for monsoons in a warmer world? Clim Change 104:403–414

Shahid S, Behrawan H (2008) Drought risk assessment in the western part of Bangladesh. Nat Hazards 46:391–413

Siqueira JR, Machado LAT (2004) Influence of the frontal systems on the day-to-day convection variability over South America. J Clim 17:1754–1766

Skansi MM, Brunet M, Sigró J, Aguilar E and others (2013) Warming and wetting signals emerging from analysis of changes in climate extreme indices over South America. Global Planet Change 100:295–307

Soares W, Marengo J (2009) Assessments of moisture fluxes east of the Andes in South America in a global warming scenario. Intern J Clim 29:1395–1414

Solman SA, Pessacg NL (2012) Evaluating uncertainties in regional climate simulations over South America at the seasonal scale. Clim Dyn 39:59–76

Solman SA, Sanchez E, Samuelsson P, da Rocha RP and others (2013) Evaluation of an ensemble of regional climate model simulations over South America driven by the ERA-Interim reanalysis: model performance and uncertainties. Clim Dyn 41:1139–1157

Torres RR, Marengo JA (2013) Uncertainty assessments of climate change projections over South America. Theor Appl Climatol 112:253–272

Editorial responsibility: Enrique Sanchez (Guest Editor), Toledo, Spain

Submitted: June 16, 2015; Accepted: March 9, 2016
Proofs received from author(s): April 29, 2016